

December 4, 2004
Biocomplexity Faculty Search Committee,
c/o Prof. Rob de Ruyter van Steveninck,
Department of Physics, Indiana University,
Swain Hall West 117,
Bloomington IN, 47405-7105

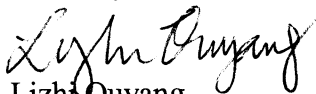
Dear Professor Steveninck,

This is Dr. Lizhi Ouyang writing in response to the "Junior Faculty Position in Biocomplexity" position posted on AIP career services. Under the guidance of Professor Wai-Yim Ching, I received my interdisciplinary Ph.D. degree in Physics and Chemistry from the Physics Department of the University of Missouri-Kansas City (UMKC) in 2000. I continued as Postdoc researcher and computational laboratory manager in Dr. Ching's Electronic Structure Group. In the meantime, I obtained my MS degree in Computer Science in 2001. I am now a research assistant professor at the Physics Department of the University of Missouri-KC. The focus of my past and ongoing research has been on the large scale first principles simulation of complex systems such as vitamin B₁₂ and its derivatives and interfaces in ceramics and biomaterials. I have had about 30 publications on quality journals such as Phys. Rev. Lett., J. of Am. Ceram. Soc., App. Phys. Lett., etc. I have collaborated and co-authored with many scientists, mostly experimentalist, from US, Japan, Italy, Canada, etc. Besides managing facilities in our own laboratory, I am in charge of the Sun Enterprise Server in the computer science department of UMKC. I also actively participate in teaching and supervising graduates students and teaching undergraduate courses. I taught General Physics II for non-science major in 2003. Together with Paul Rulis, the graduate student working under my supervision, I built the first PC cluster on campus in 1998. I enjoy teaching and interacting with fellow students and always view it as mutual beneficial.

Included are my curriculum vita, teaching and research statements and three copies of my recent publications. For your convenience I list five references in a separate page.

Hiring a tenure track assistant professor is long term commitment and I am committed to this academic career. I am confident that I am well prepared and up to the challenges lying ahead. Thank you for your considerations and I am looking forward to hearing from you.

Sincerely,



Lizhi Ouyang
Research Assistant Professor
Department of Physics
University of Missouri-KC
5110 Rockhill Rd
Kansas City, MO 64110
Tel: (o)816-235-1058/2512 (h) 913-901-8413
Email: ouyangl@umkc.edu

Lizhi Ouyang's Research Statement

My goal is to understand interfacial properties of ceramics and biomaterials by means of computer simulation. Interface at nano-scale is of great importance to modern science and technologies. Yet comprehensive understanding of these interfaces has remained elusive, largely due to their nanoscale sizes and heterogeneous structures that render current techniques difficult if not impossible to elucidate the structure-property relations. While experimental techniques such as ELNES/XANES, Micro-Raman, X-ray diffraction, Sum Frequency Generation (SFG), *etc.* can be used to obtain the compositions, average coordinations, local bondings of the films, these scattered informations have yet to be consolidated to retrieve the structural informations of the thin films. With the fast advance of computer technologies, "numeric experiments" carry out by the state-of-the-art computer simulations techniques nowadays can produce "measurements" for systems of hundreds or even thousands of atoms with considerable accuracy. However, the heterogeneity at nano/meso scale such as those found in Si_3N_4 and bone tissue presents a formidable challenge to "numeric experiments" before of the size of models required to properly describe the materials. The main thrust of my current research is to develop and apply multiscale simulation methods to model the structures of the nano thin film and bio-materials and to compute their physical properties.

Selected Current Researches

1. *Electronic Structure and Bonding of B_{12} and its derivatives (Supported under DOE grant #DE-FG02-94DR45170, Amount: \$487K [07/02-06/05])*

B_{12} is a vital substance for the rapid synthesis of DNA during cell division. Being the most complex vitamin and nature's only bio-molecule with a Co-C bond, B_{12} has attracted wide research interests. We, for the first time, using structures accurately determined from X-ray diffraction, calculated the electronic structures and bonding of a whole B_{12} by first principles methods. Our partial density of states calculations agree well with X-ray absorption spectra. Our calculations also elucidate the origins of several pronounced peaks in the vis/UV absorption spectra. Based on past research, I am in preparation to submit a proposal to NSF biomolecular program in Jan, 2005. The goal of the proposal is to investigate the evolving of XANES of Co in B_{12} during Co-C bond breaking.

2. *Nanometer Scale Induced Structure Between Amorphous Layers and Crystalline Materials (NANOAM) (NSF#DMR-0016, Amount: \$2.1M [06/01-08/05])*

I have participated in the NANOAM project, a jointly funded collaboration between the US-NSF -and the European Community. The topics I have been involved include:

- a. *Structural and dielectric properties of high-k dielectric materials Zr silicate ($\text{Zr}_x\text{Si}_{2-x}\text{O}_4$).* Using first principles methods, we have calculated the dielectric properties of Zr silicate with varying Zr content by considering the Zr silicate as regular solution in zircon lattice structure. We found that low x Zr silicate show better compatibility with the substrate and significant increase of dielectric constant. We also found that surprisingly, the structure of pure SiO_2 at $x=0$ can be reduced to an inverse Ag_2O structure which we found to be new metastable phase of SiO_2 that has a high static dielectric constant of about 10. We are currently extended this work to amorphous Zr silicate models.
- b. *Modeling of Si_3N_4 intergranular thin film.* We are the first to perform first principles calculations on realistic atomic models of intergranular thin film. We results verified the validity of empirical potential methods in regions away from structural discontinuities and demonstrated the necessity of involving accurate first principles methods through either directly modeling or indirectly, improving the empirical potential to count for the structural discontinuity. We are current analysis the results to test against two proposed theories about the origin the consistent thin film thickness of about 1nm in Si_3N_4 intergranular thin film.

Future Research Plans

The direction of my future research is on bio-inspired materials. Together with UMKC dental school and school of computer engineering, we have recently submitted a proposal to National Institute of Biomedical Imaging and Bioengineering (NIBIB). I am intensively involved in two topics:

1. Investigating the buried mineral-collagen interfacial structures in biomaterials such as bone and teeth. Currently the biggest problem with artificial implants lies in the tissue-implant interface which shows distinct differences from natural ones. The nature tissue is organized in a hierarchic manner which shows heterogeneity at micro, nano/meso and macro-scale. Thus it requires understandings at each level to better engineer the artificial implant. Among the structural hierarchy of nature tissues, the interface between mineral crystallites and soft tissues (mostly collagen fibrils) where the nature's own engineering, the biomineralization process happens, is a very important yet an extremely complicated one. Topics pertaining to the mineral-collagen interface include understanding the bonding or cross-link between the minerals and collagen fibrils; understanding the role of bonded the water in the mineral-collagen interface; understanding the mechanism control the growth of the mineral crystallites. I plan to use first-principles calculations coupling with classical molecular dynamics to study the above topics. Proper description of the mineral-collagen interface requires at least hundreds of atoms or more. Fortunately, calculating systems with thousands of atoms using first principles methods based density functional theory is now possible with modern computer. In fact, I have in the past study an 800 atoms Si_3N_4 intergranular thin films model using Vienna ab initio Simulation Package and first-principles Orthogonalized linear combination atomic orbitals program.

2. Developing an open, component based, problem-solving oriented software infrastructure for seamless integration of various simulation packages targeted at specific scales to perform multiscale simulations through software engineering. The key to multiscale simulation integration is the seamless exchange of input/output parameters so that smaller scales simulation could provides input to larger scale simulations and results from larger scale simulations could provide feedbacks to smaller scale simulations. The lack of standard for even the basic parameters such as geometry has so far hindered the development of generic multiscale simulation solutions. Our solution to this problem is to separating the underlying physics from its implementation or so-called data abstraction. To do so, I propose to create a common "language" through which any simulation program can "talk" to each other. We plan to implement the common "language" using the EXtensible Markup Language (XML), a way to generically describe data to facilitate data exchange that are widely used in many commercial software and academic researches.

Computational Facilities

I am experienced in design, build and maintain computer clusters and SAN storage networks; maintain Sun Enterprise Server, Alpha workstations, etc. If financially permitted, I will build an inexpensive yet reliable out-of-shelf cluster computer for research and hands on trainings purpose. My experiences show that the involvement of undergraduate students can be very beneficial in that the provided first hand experience of high performance computing could attract well-motivated students into this interdisciplinary research area.

I am a frequent user of national super computer facilities at National National Energy Research Scientific Computing Center and other DOE facilities. I was recently awarded 10,000 PSU of NSF supercomputer time to calculate the X-ray Absorption Near Edge Structure (XANES) of B_{12} derivatives using Slater's transition state theory.

Collaborators

Prof. W.Y. Ching, University of Missouri-Kansas City, USA (supervisor, co-author)

Prof. Lucio Randaccio, University of Trieste, Italy, (collaborator, co-author)

Prof. Alexander Moewes, University of Saskatchewan, Canada (collaborator, co-author)

Prof. Ernst Kurmaev, Institute of Metal Physics, Russia Academy of Scinces, Russssia (co-author)

Prof. D.M. Zhu, University of Missouri-Kansas City, USA (collaborator, co-author)

Prof. Isao Tanaka, Kyoto Univeristy, Japan (collaborator, co-author)

Prof. Paulette Spencer, University of Missouri-Kansas City, USA (collaborator)

Prof. K.W. Wong-Ng, National Institute of Standard and Technology, USA (collaborator, co-author)

Prof. Stephen Garofalini, Rutgers University, USA (collaborator, co-author)

Prof. Yet-Ming Chiang, Massachusetts Institute of Technology, USA (collaborator)

Prof. Roger R. French, Du pont Co. USA (collaborator)

Lizhi Ouyang's Teaching Statement

I prefer to use Socratic methods in the classroom because I believe a good teacher is who can inspire the student to ask a good question. The ability to ask a good question is the key step toward understanding and a clear indication of self-instructions. My experience as lecturer for general physics convinced me that teacher can not teach the student much within the limited interactions with the student. Instead, they can only motivate students to teach themselves. My role as a teacher is to dispel the “mysteries” of physics and help the students to formulate a good question and then introduce the problem-solving techniques which often become apparent. There are ample examples in the literatures demonstrating large varieties of ways to stimulate active learning and encourage and induce the student to ask question. My most favorable way is to know my student and also have the student know me so that we all can be comfortable in the classroom. I would like to make it clear to the student that every question is a good question and being wrong is the part of learning. Good ways to know my students include inviting student to my office for conversation; periodical evaluation; organizing relevant after-class program involved students and myself, etc. I will also leverage my expertise of being a linux veteran and a computer hardware guru to attract students.

I highly value hand-on experiences in teaching physics. Hand-on experiences help reinforce the concepts learned in classroom by materializing those abstract concepts in a more intuitive way. Having students in contact with the state-of-the-art computational facilities will simulate their interests and make them better prepared for their future career. Besides after-class homework and projects, in class physical and computer demonstrations is my favorite approach to give students hands-on experience.

With a master degree in computer science, I am quite effective in using computers to aid my teaching. I developed websites for my classes as an interface to engage the students. Discussion forums and instant messages are my favorite tools to communicate with students. To encourage the students to participate, I have students themselves act as moderators on the discuss forums. While I am delighted to using modern technologies to aid my teaching, I also learned from my experience that students still enjoy the traditional classroom with a whiteboard and a marker. It is easier for students to following my thinking in a traditional classroom. And, unlike a pre-designed slide show, I can also adjust my teaching on-the-fly according to the responses of my students.

I am interested in developing courses specific to my research interest and expertise, *parallel computing and quantum mechanic simulations*. The course, using the current state-of-the-art open source programs such as ABINIT and PWscf and my own code of Orthogonalized Linear Combination of Atomic Orbitals methods (OLCAO) as tools, will introduce the theories and algorithms behinds them and trade-offs and limitation of these approaches. Implementation practices such as messaging passing interface (MPI), data decomposition, will also be addressed in the courses. I will specifically emphasize on hand-on experiences by making student projects an integrate part of the course.

Accurate Redetermination of the X-ray Structure and Electronic Bonding in Adenosylcobalamin

Lizhi Ouyang, Paul Rulis, and W. Y. Ching*

Department of Physics, University of Missouri—Kansas City, Kansas City, Missouri 64110

Giorgio Nardin and Lucio Randaccio*

Centre of Excellence in Biocrystallography—Department of Chemical Sciences, University of Trieste, 34127 Trieste, Italy

Received July 18, 2003

The electronic structure of adenosylcobalamin (B_{12} coenzyme, AdoCbl) has been calculated by a density functional method, using the orthogonalized linear combination of the atomic orbital method (OLCAO). Since a fixed accurately determined geometry was needed in such calculations, the crystal structure of adenosylcobalamin has been redone and refined to $R = 0.065$, using synchrotron diffraction data. Comparison with the recently reported electronic structures of cyano- (CNCbl) and methylcobalamin (MeCbl) shows that the net charges and bond orders vary only on the axial donors. The values in the three cobalamins suggest that the Co–C bond in MeCbl has a strength similar to that in AdoCbl, but it is significantly weaker than that in CNCbl. Present results are compared with those previously reported for the analogous corrin derivatives; i.e., simplified cobalamins with the side chains a–f replaced by H atoms. Despite a qualitative agreement, a discrepancy in the calculated HOMO–LUMO gap is found.

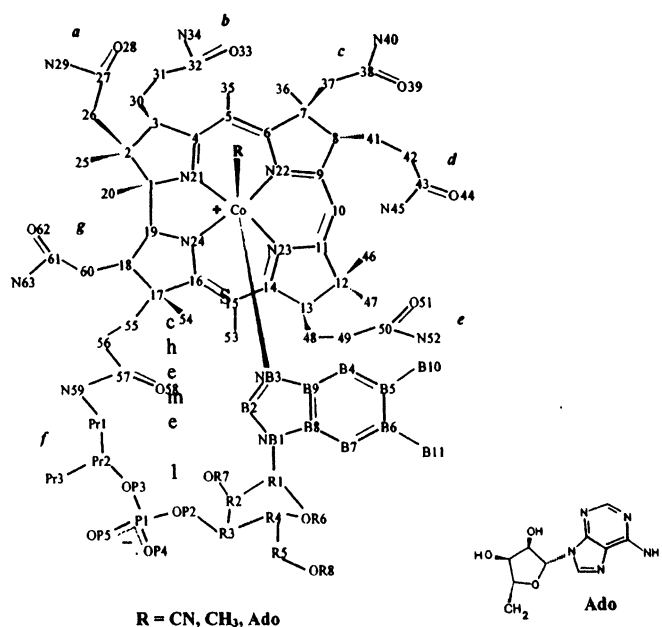
Introduction

The B_{12} cofactors so far known are alkylcobalamins (RCbl) consisting of a cobalt corrinoid with a pendant nucleotide (with different purine base), which occupies five of the six coordination sites of an octahedral Co(III). The sixth position is occupied by the R group or by a CN ligand in the cyanocobalamin (CNCbl), the vitamin B_{12} itself (Scheme 1). CNCbl is not a biologically active species, whereas the cobalamins having $R =$ methyl (methylcobalamin, MeCbl) and 5'-deoxy-5'-adenosyl (coenzyme B_{12} , AdoCbl) are cofactors of several enzymes. All the currently known reactions of B_{12} -dependent enzymes involve the making and breaking of the Co–C bond.¹

The MeCbl-based enzymes (methyltransferases) catalyze the transfer of methyl groups, and the overall mechanistic scheme requires a reversible *heterolytic* cleavage of the Co–Me bond.²

The process catalyzed by AdoCbl-based enzymes (isomerase and eliminase) proceeds through a stepwise process initiated

Scheme 1

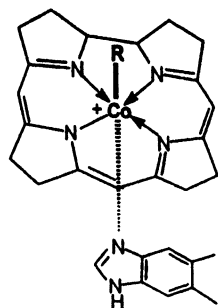


* To whom correspondence should be addressed. E-mail: randaccio@univ.trieste.it (L.R.).

- (1) *Vitamin B₁₂ and B₁₂ Proteins*; Kräutler, B. D., Arigoni, B. D., Golding, B. T., Eds.; Wiley-VCH: Weinheim, 1998. *Chemistry and Biochemistry of B₁₂*; Banerjee, R., Ed.; J. Wiley & Sons: New York, 1999.
- (2) Matthews, R. G. *Acc. Chem. Res.* **2001**, *34*, 681–689.

by the *homolytic cleavage* of the Co–C bond.³ The homolysis rate in the enzyme is increased by a factor of about 10^{12} , with respect to the free coenzyme. How such a spectacular

Scheme 2



acceleration is achieved by the interaction with the apoenzyme is a subject of debate and is not adequately understood at present.³ The first structural determinations of B₁₂ enzymes (isomerase and methyltransferase)⁴ indicated that the benzimidazole moiety (Scheme 1) moves away from cobalt (base-off form) and is replaced by a histidine residue of the protein. Thus, this was thought to be related in some way to the homolysis acceleration. However, the X-ray structure of an eliminase has recently shown that no benzimidazole displacement occurs in this enzyme.⁵

It is clear that the understanding of the factors influencing the Co–C bond cleavage also requires an in-depth study of the electronic structure and bonding in cobalamins. Detailed knowledge of the electronic properties of the Co–C bond should also be instrumental in answering some additional basic questions, such as which factors determine the different behavior of MeCbl and AdoCbl toward the Co–C cleavage? Accurate theoretical calculations on the isolated coenzymes should, in principle, reveal the specific electronic features that discriminate the Co–Me and Co–Ado bonds. Furthermore, the physicochemical properties, such as spectroscopic data, of such biomolecules appear somewhat conflicting^{6–9} and could find an explanation on firm theoretical grounds.

Theoretical calculations were attempted in the past on simple models¹⁰ and on the positively charged RCo–corrin (Scheme 2), which are simplified cobalamins with the side chains a–f (Scheme 1) replaced by the H atoms. These studies^{11,13} were based on semiempirical approaches and

sometimes reached conflicting conclusions. Only recently has the density functional theory (DFT) been applied to alkyl-corrin complexes, with a dramatic increase in the number of papers.^{14,15} However, accurate geometric parameters of the molecule are very important for the linear combination of the atomic orbital (LCAO) method. Until a few years ago, structural data on cobalamins were of low accuracy, preventing meaningful comparison. The structure of the B₁₂ coenzyme has been extensively studied by means of X-ray¹⁶ and neutron diffraction.¹⁷ However, these studies did not attain an accuracy dramatically better than those obtained by Lenhert in the early structural determination.¹⁸ Therefore, Kratky and Kräutler stated¹⁹ that it is highly desirable that an X-ray high-resolution structure of the coenzyme B₁₂ become available. Analogously, a low-resolution structure of MeCbl was reported many years ago.²⁰ Only recently, thanks to the use of the synchrotron X-ray source coupled with area detectors (for high-speed data collection) as well as improvement in the crystallization techniques, has accurate structural data of several cobalamins been obtained,²¹ including the redetermination of CNCbl and MeCbl.²²

On the basis of these accurate structural data, we have recently calculated the electronic structure of CNCbl²³ and MeCbl²⁴ by a first-principles method using for the first time the complete cobalamin molecule including the side chains (Scheme 1). These calculations have been found fully consistent with UV–vis, XES, and XPS experimental data. Now, we extend this theoretical approach to the complete molecule of AdoCbl. Since our DFT approach requires fixed

- (3) Marzilli, L. G. In *Bioinorganic Catalysis*; Reedijk, J., Bouwman, E., Eds.; Marcel Dekker: New York, 1999; pp 423–468.
- (4) Drennan, C.; Huang, S.; Matthews, R. G.; Ludwig, M. L. *Science* **1994**, *266*, 1669–1674. Mancia, F.; Keep, N. J.; Nakagawa, A.; Leadly, P. F.; McSweeney, S.; Rasmussen, B.; Bosecke, P.; Diat, P.; Evans, P. R. *Structure* **1996**, *4*, 339–350.
- (5) Shibata, N.; Masuda, J.; Tobimatsu, T.; Toraya, T.; Suto, K.; Morimoto, Y.; Yasuoka, N. *Structure* **1999**, *7*, 997–1008.
- (6) Dong, S.; Padmakumar, R.; Banerjee, R.; Spiro, T. G. *J. Am. Chem. Soc.* **1996**, *118*, 9182–9183. Dong, S.; Padmakumar, R.; Maiti, N.; Banerjee, R.; Spiro, T. G. *J. Am. Chem. Soc.* **1998**, *120*, 9947–9948. Dong, S.; Padmakumar, R.; Banerjee, R.; Spiro, T. G. *J. Am. Chem. Soc.* **1999**, *121*, 7063–7070.
- (7) Puckett, J. M., Jr.; Mitchell, M. B.; Hirota, S.; Marzilli, L. G. *Inorg. Chem.* **1996**, *35*, 4656–4662.
- (8) Hay, B. P.; Finke, R. G. *J. Am. Chem. Soc.* **1987**, *109*, 8012–8018.
- (9) Kumar, M.; Qiu, D.; Spiro, T. G.; Ragsdale, S. W. *Science* **1995**, *270*, 628–630.
- (10) Christianson, D. W.; Lipscomb, W. N. *J. Am. Chem. Soc.* **1985**, *107*, 2682–2686. Hansen, L. M.; Pavan Kumar, P. N. V.; Marynick, D. S. *Inorg. Chem.* **1994**, *33*, 728–735. Mealli, C.; Sabat, M.; Marzilli, L. G. *J. Am. Chem. Soc.* **1987**, *109*, 1593–1594.
- (11) Zhu, L.; Kostic, N. M. *Inorg. Chem.* **1987**, *26*, 4194–4197.
- (12) Hansen, L. M.; Derecskei-Kovacs, A.; Marynick, D. S. *J. Mol. Struct.* **1998**, *431*, 53–57.
- (13) Rovira, C.; Kunc, K.; Hutter, J.; Parrinello, M. *Inorg. Chem.* **2001**, *40*, 11–17.
- (14) (a) Andruniow, T.; Zgierski, M. Z.; Kozlowski, P. M. *J. Phys. Chem. B* **2000**, *104*, 10921–10927. (b) Randaccio, L.; Geremia, S.; Nardin, G.; Stener, M.; Toffoli, D.; Zangrando, E. *Eur. J. Inorg. Chem.* **2002**, 93–103. (c) Jensen, K. P.; Saur, S. P. A.; Liljefors, T.; Norrby, P. O. *Organometallics* **2001**, *20*, 550–556. (d) Jensen, K. P.; Ryde, U. *J. Phys. Chem. A* **2003**, *107*, 7539–7545. (e) Dölker, N.; Maseras, F.; Lledos, A. J. *J. Phys. Chem. B* **2003**, *107*, 306–315. (f) Andruniow, T.; Zgierski, M. Z.; Kozlowski, P. M. *J. Chem. Phys.* **2002**, *115*, 7522–7533. (g) Jensen, K. P.; Ryde, U. *J. Mol. Struct. (THEOCHEM)* **2002**, *585*, 239–255.
- (15) (a) Andruniow, T.; Zgierski, M. Z.; Kozlowski, P. M. *J. Am. Chem. Soc.* **2001**, *123*, 2679–2680. (b) Andruniow, T.; Zgierski, M. Z.; Kozlowski, P. M. *J. Phys. Chem. A* **2002**, *106*, 1365–1373.
- (16) Savage, H. F. J.; Finney, J. L. *Nature* **1986**, *322*, 717–720. Savage, H. F. J.; Lindley, P. F.; Finney, J. L.; Timmins, P. A. *Acta Crystallogr., Sect. B* **1987**, *B43*, 280–295.
- (17) Bouquiere, J. P.; Finney, J. L.; Savage, H. F. J. *Acta Crystallogr., Sect. B* **1994**, *B50*, 566–578. Bouquiere, J. P.; Finney, J. L.; Lehmann, M. S.; Lindley, P. F.; Savage, H. F. J. *Acta Crystallogr., Sect. B* **1993**, *B49*, 79.
- (18) Lenhert, P. G. *Proc. R. Soc. London, Ser. A* **1968**, *A303*, 45–84.
- (19) Kratky, C.; Kräutler, B. In *Chemistry and Biochemistry of B₁₂*; Banerjee, R., Ed.; J. Wiley & Sons: New York, 1999; pp 9–41.
- (20) Rossi, M.; Glusker, J. P.; Randaccio, L.; Summers, M. F.; Toscano, P. J.; Marzilli, L. G. *J. Am. Chem. Soc.* **1985**, *107*, 1729–1738.
- (21) Kratky, C.; Färber, G.; Gruber, K.; Deuter, Z.; Nolting, H. F.; Konrat, R.; Kräutler, B. *J. Am. Chem. Soc.* **1995**, *117*, 4654–4670. Brown, K. L.; Cheng, S.; Zubkowski, J. D.; Valente, E. J.; Kropton, L.; Marques, H. M. *Inorg. Chem.* **1997**, *36*, 3666–3675. Randaccio, L.; Furlan, M.; Geremia, S.; Slouf, M. *Inorg. Chem.* **1998**, *37*, 5390–5393. Randaccio, L.; Geremia, S.; Nardin, G.; Slouf, M.; Smova, I. *Inorg. Chem.* **1999**, *38*, 4087–4092.
- (22) Randaccio, L.; Furlan, M.; Geremia, S.; Slouf, M.; Smova, I. *Inorg. Chem.* **2000**, *39*, 3403–3413.
- (23) Ouyang, L.; Randaccio, L.; Rulis, P.; Kurmaev, E. Z.; Moewes, A.; Ching, W. Y. *J. Mol. Struct.* **2003**, *622*, 221–227.
- (24) Kurmaev, E. Z.; Moewes, A.; Ouyang, L.; Randaccio, L.; Rulis, P.; Ching, W. Y. *Europhys. Lett.* **2003**, *62*, 582–587.

Table 1. Crystal Data and Structure Refinement for AdoCbl

formula	C ₇₂ H ₁₀₀ CoN ₁₈ O ₁₇ P·1.25(C ₂ H ₆ O)·8.25(H ₂ O)
fw	1800.83
T, K	100(2)
λ, Å	0.737
cryst syst; struct group	orthorhombic; P2 ₁ 2 ₁ 2 ₁
a, Å	15.194(15)
b, Å	21.32(2)
c, Å	27.55(3)
V, Å ³	8923(16)
Z; ρ _{calcd} , Mg/m ³	4; 1.341
μ, mm ⁻¹	0.295
F(000)	3834
crystal size, mm	0.20 × 0.20 × 0.50
refinement method	full-matrix least squares on F ²
data/restraints/params	19149/0/1113
goodness-of-fit on F ²	1.001
final R indices [I > 2σ(I)]	R1 ^a = 0.066, wR2 ^b = 0.187
R indices (all data)	R1 = 0.067, wR2 = 0.188

$$^a R1 = \sum ||F_o| - |F_c|| / \sum |F_o|. \quad ^b wR2 = [\sum w(|F_o|^2 - |F_c|^2)^2 / \sum w|F_o|^2]^{1/2}.$$

highly accurate structural data, the X-ray analysis of AdoCbl based on synchrotron data is also reported.

Experimental Section

Crystallization. Commercial samples of AdoCbl, with a stated purity by the manufacturer of about 98%, were from Fluka. Several attempts to grow single crystals by the hanging drop method under different conditions²² led to red parallelepiped-shaped crystals, some of which were used to collect diffraction data. However, the subsequent data analysis showed that these crystals were of low quality. By contrast, successive attempts to grow single crystals by slow evaporation of AdoCbl water solution after the addition of acetone were successful, and one of these crystals was used for the final data collection.

X-ray Data Collection and Crystal Structure Refinement. Data collection was carried out at the X-ray diffraction beamline of the Elettra synchrotron (Trieste, Italy) using the rotating crystal method and a 345 mm Mar image plate. Crystals were mounted in a loop and frozen to 100 K, using a nitrogen stream cryocooler. Intensity data were processed using the program DENZO and scaled and merged using the program SCALEPACK.^{25a} Friedel pairs were not merged (anomalous dispersion included), and no absorption correction was applied. The structure was solved starting from the previously determined coordinates and refined by the full-matrix least-squares method using SHELXL-97.^{25b} Crystal data and structure refinement details are displayed in Table 1.

Theoretical Method. The electronic structure of AdoCbl, using the newly determined structure, was calculated by the ab initio orthogonalized linear combination of the atomic orbital method (OLCAO)²⁶ based on the density functional theory (DFT)²⁷ in its local density approximation (LDA).²⁸ Similar calculations for CNCbl and MeCbl have been reported.^{23,24} The OLCAO method is an all-electron method particularly suitable for large complex crystals and molecules. In the OLCAO method, the basis functions are expanded in terms of atomic orbitals, which are themselves

formed as linear combinations of Gaussian-type orbitals (GTO). The LDA potential is constructed from the total charge density and is conveniently written as a sum of atom-centered functions, which also consist of GTOs. This facilitates the evaluation of various types of multicenter integrals with no limitations on their ranges of interaction. There are several special advantages to the OLCAO method. First, the orthogonalization to the core procedure (or the frozen core approximation) reduces the dimension of the final secular equation and speeds up the self-consistent iterations, making it applicable to complex biomolecular systems of up to thousands of atoms. Second, the atomic description of the basis function allows us to use the Mulliken scheme²⁹ to resolve the total density of states (DOS) into atom- and orbital-resolved (or even spin-resolved) partial components, or partial DOS (PDOS). The PDOS is a concept widely used in solid-state physics, and provides information on the number of energy states per unit range of energy and the parentage of the state. The PDOS for each individual atom or a group of atoms in a complex molecule is particularly useful because it can pinpoint the complicated interatomic and intermolecular interactions of specific functional groups in a graphic form. The PDOS result can be compared with experimental data from resonant X-ray photoemission spectra, which explore the valence band states of the molecule, as was demonstrated in refs 23 and 24. Third, the Mulliken scheme can also provide effective atomic charge Q_α^* on atom α , and bond order $\rho_{\alpha,\beta}$ between pairs of atoms (α and β) which are defined as

$$Q_\alpha^* = \sum_i \sum_{n,occ} \sum_{j\beta} C_{i\alpha}^n C_{j\beta}^n S_{i\alpha,j\beta} \quad (1)$$

$$\rho_{\alpha,\beta} = \sum_i \sum_j C_{i\alpha}^n C_{j\beta}^n S_{i\alpha,j\beta} \quad (2)$$

In eqs 1 and 2, $C_{i\alpha}^n$ is the eigenvector coefficients of the n th state; $S_{i\alpha,j\beta}$ is the overlap integral between wave functions with atomic specifications of α and β and orbital specifications of i and j . Q^* is the total number of electrons on the α atom. The effective charges provide information on atomic charge transfer, and the bond order is a quantitative measure of the strength of the bond between a pair of atoms. Since Mulliken analysis is more accurate when the basis functions are localized, it is customary to calculate Q_α^* and $\rho_{\alpha,\beta}$ using a separate minimal basis set calculation. The net charge on atoms are calculated by subtracting Q^* from the number of their valence electrons.

On the basis of the accurately determined crystal structures, the electronic structure of AdoCbl molecule was calculated using the OLCAO method. In contrast to previous theoretical investigations on Co (corrin),^{14,15} the present calculation includes all the atoms in the side chain of the molecule. An extended basis set consisting of atomic orbitals of Co (1s,2s,2p,3s,3p,4s,4p,3d, 5s,5p,4d), C, N, and O (1s,2s,2p,3s,3p), P (1s,2s,2p,3s,3p,4s,4p,3d), and H (1s,2s,2p) was adopted. Then, the secular equation has a dimension of 1387. More than 60 iterations are needed to have a fully converged self-consistent potential when the eigenvalues stabilize to within 0.00001 eV.

Results

X-ray Structure. X-ray analysis showed that the acetone content per Co atom is 1.25 as compared with that of 0.15

- (25) (a) Otwinowski, Z.; Minor, W. *Methods Enzymol.* **1996**, *276*, 307.
 (b) Sheldrick, G. M. *SHELXL-97*; Universität Göttingen: Göttingen, 1997.
 (26) Ching, W. Y. *J. Am. Ceram. Soc.* **1990**, *73*, 3135–60. Ching, W. Y. In *The Magnetism of Amorphous Metals and Alloys*; Fernandez-Baca, J. A., Ching, W. Y., Eds.; World Scientific: Singapore, 1995; pp 85–141.
 (27) Hohenberg, P.; W. Kohn, W. *Phys. Rev. B* **1964**, *136*, B864–B871.
 (28) Kohn, W.; Sham, L. J. *Phys. Rev.* **1965**, *140*, A1131–1138. Sham, L. J.; Kohn, W. *Phys. Rev.* **1966**, *145*, 561–567.

- (29) Mulliken, R. S. Electron Population Analysis on LCAO-MO Molecular Wave Functions. I. *J. Am. Chem. Soc.* **1955**, *23*, 1833–1840. Mulliken, R. S. Electron Population Analysis on LCAO-MO Molecular Wave Functions. II. *J. Am. Chem. Soc.* **1955**, *23*, 1841–1846.

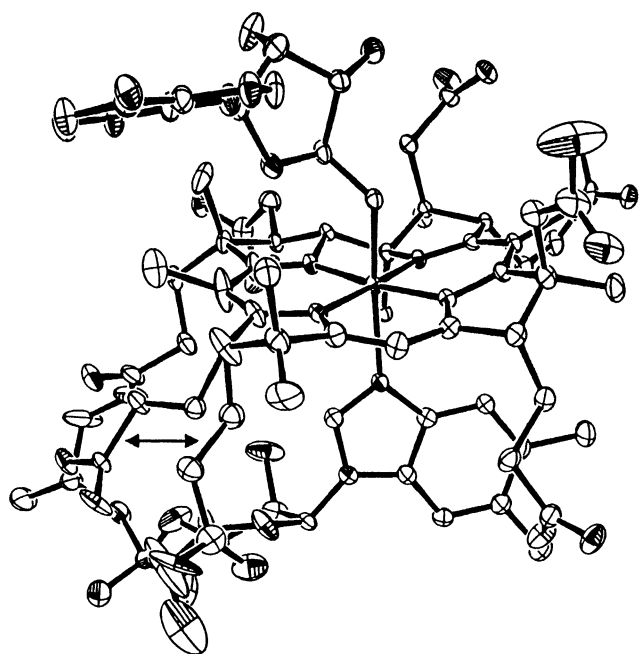


Figure 1. ORTEP drawing of AdoCbl. Atoms are drawn at the 30% probability level. The two orientations of the ϵ chain are both reported and indicated by the double arrow.

detected in the AdoCbl crystal structure, determined by neutron diffraction at 15 K.¹⁶ However, the unit cell parameters are very similar.

An ORTEP drawing of AdoCbl is shown in Figure 1. The superimposition of the non-H atom skeletons of AdoCbl, obtained from neutron and X-ray data, is shown in Figure 2. They superimpose quite well, with only some conformational changes involving the adenosyl and ribosyl moieties and the ϵ amide chain (Scheme 1). In the present structure the latter has two distinct conformations with half-occupancy each. One of the two conformations superimposes well with that found in the neutron structure. This conformational difference should be attributed to the different acetone content. In fact, the acetone molecule with half-occupancy (the other having 0.75 occupancy) is located in the same region where one of the two conformations of chain ϵ is located.

The coordination bond lengths and angles in the present structure do not differ dramatically from those previously reported,^{16,30} as well as the Co-CH₂-C angle (Table 2). However, that the accuracy (as measured by the estimated standard deviations on distances) of the AdoCbl X-ray structure is higher than the neutron one can be appreciated.

The axial distances and some other physicochemical properties of CNCbl, MeCbl, and AdoCbl are compared in Table 2. These data show that there are significant differences in the geometry of the axial fragment, in ground-state physicochemical properties, and in the half-wave potentials, $E_{1/2}$, between the two coenzymes. On the other hand, it has been shown that the Co-N equatorial distances are essentially unaffected by the change in the axial R ligand.³⁰

(30) The two short Co-N21 and Co-N24 distances^{21,22} average to 1.876 (4) Å in both coenzymes, and the two long Co-N22 and Co-N23 ones average to 1.920 (4) and 1.915 (3) Å in MeCbl and AdoCbl, respectively.

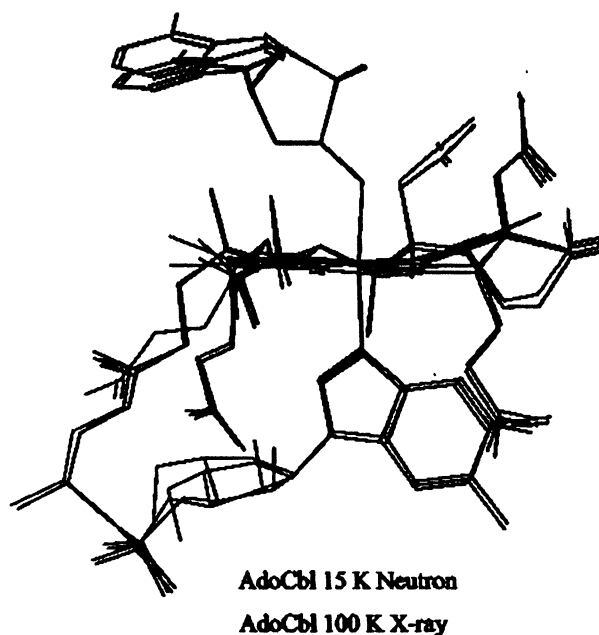


Figure 2. Superimposition of AdoCbl skeletons from neutron (red) and X-ray (black) data. One of the two orientations of the ϵ chain is in blue.

Comparison of data in Table 2 shows the following:

(i) There is a significant lengthening of the Co-N bond in AdoCbl, indicating that Ado exerts a trans influence greater than that of Me.

(ii) The Co-C bond is appreciably lengthened in AdoCbl. Correspondingly, the $\nu_{\text{Co-C}}$ frequency and the Co-C bond dissociation energy (BDE) decrease. Therefore, the Co-C bond in AdoCbl should be weaker than that in MeCbl. The weakening appears to be related to the larger bulk of the Ado group, which is only partially released by the unusual opening of the Co-C(sp³)-C angle up to 123°. However, a contribution to this lengthening (weakening), due to the different electronic properties of Ado and Me, cannot be ruled out, as suggested in simple models.³¹

(iii) The lengthening of the axial distances in AdoCbl with respect to MeCbl corresponds to a less negative value of $E_{1/2}$, i.e., to a less electron rich cobalt center.

The above experimental evidence supports the notion that the Co-C bond in MeCbl is stronger than that in AdoCbl. However, it does not find correspondence in the results of theoretical calculations described below.

Theoretical Calculations. Recent DFT theoretical calculations on corrins focused on factors which could enhance the Co-C homolysis. Optimization of the geometry of R-Co-corrin-base (with several R and L axial base ligands), confirmed¹⁴ spectroscopic data^{6,7} that variation of L has little effect on the Co-C bond. Calculations indicate that Ado(corrin)L has ca. 5 kcal/mol higher HOMO and LUMO energy with respect to the methyl analogue, when L = 5,6-dimethylbenzimidazole (bzm). This finding was claimed to be a theoretical explanation as to why AdoCbl undergoes homolysis more easily and MeCbl undergoes heterolysis more easily.^{14c}

(31) Randaccio, R.; Geremia, S.; Zangrando, E.; Ebert, C. *Inorg. Chem.* 1994, 33, 4644-4650.

Electronic Structure of Adenosylcobalamin

Table 2. Comparison of Some Geometric Parameters (esd's in Parentheses), and Spectroscopic, Electrochemical and Thermodynamic Properties of the Axial Fragment in MeCbl, AdoCbl, and CNCbl

	Co-C (Å)	Co-NB3 (Å)	Co-C-C (deg)	$\nu_{\text{Co-C}}$ (cm ⁻¹)	$E_{1/2}^b$ (V)	BDE ^c
MeCbl	1.979 (4) ^d	2.162 (4) ^d		506	-1.60	37 ± 3
AdoCbl (X-ray)	2.030 (3) ^e	2.237 (3) ^e	123.4 (2) ^f	430	-1.35	30 ± 2
AdoCbl ^g (neutron)	2.023 (10)	2.214 (9)	122.6			
CNCbl ^d	1.886 (4)	2.041 (3)	180.0 (1)			

^a Reference 6; data were obtained with resonance Raman spectroscopy. A similar value of 500 cm⁻¹ for crystalline MeCbl was obtained by Fourier transform Raman spectroscopy (Nie, S.; Marzilli, P. A.; Marzilli, L. G.; Yu, N. T. *J. Chem. Soc., Chem. Commun.* 1990, 770-771). ^b Lexa, D.; Saveant, J. M. *J. Am. Chem. Soc.* 1978, 100, 3220-3222. Sheperd, R. E.; Zhang, S.; Dowd, P.; Hoi, G.; Wick, B.; Choi, S. *Inorg. Chim. Acta* 1990, 174, 249-256. ^c Martin, B. M.; Finke, R. G. *J. Am. Chem. Soc.* 1992, 114, 585-592. BDE = Co-C bond dissociation energy toward homolysis in kcal/mol. ^d Reference 22. ^e Present work. ^f Reference 18.

Table 3. Net Charge (NC) on Co and Donor Atoms and BO of Coordination Bonds^a

	CNCbl ^b	MeCbl ^c	AdoCbl
NC(Co)	+0.72	+0.71	+0.71
NC(NB3)	-0.35	-0.34	-0.36
NC(C)	+0.01	-0.81	-0.58
NC(N21-24) ^d	-0.30	-0.32	-0.31
NC(N22-23) ^d	-0.36	-0.36	-0.36
BO(Co-C)	0.25	0.13	0.15
BO(Co-NB3)	0.18	0.16	0.15
BO(Co-Neq) ^d	0.21	0.23	0.23

^a NC is derived by subtracting Q^* from the number of valence electrons of the given atom. ^b Reference 23. ^c Reference 24. ^d Mean values.

However, in all the above calculations wave functions of the electronic state were not explicitly discussed. Wave function and charge distribution are important aspects of the electronic structure. In Table 3, we list the calculated Mulliken charges and bond orders in the AdoCbl molecule and compare them with the results of similar calculations on MeCbl²⁴ and CNCbl.²³ Only those atoms bonded to Co are listed.

For the net charges, we observe that (1) Co as a cation loses about 0.7 electron. (2) The net charges on the N atoms in the corrin ring (N21, N22, N23, N24) are similar. On average, each N gains about 0.33 electron. (3) The net charge of NB3 is -0.36. (4) The net charge of the C atom bonded to Co, C α , is -0.58. (5) The net charge for the C atoms in the corrin ring ranges from +0.13 to -0.33 (not listed, but very similar to those in refs 23 and 24), indicating a resonant-like character for C in the corrin ring. (4) The net charges of all the other atoms in the molecule are similar to those in CNCbl²³ and MeCbl.²⁴ (5) With the exception of the C atom bond to Co, the corresponding net charges in all three molecules are very close to each other. The situation is slightly different in the case of bond order. We find the bond order for the Co-C in AdoCbl, MeCbl, and CNCbl to be 0.15, 0.13, and 0.25, respectively. Thus, in AdoCbl, the Co-C bond order is only slightly higher than that in MeCbl and much lower than that in CNCbl. On the other hand, the bond order of Co-NB3 is only 0.15, much less than that of 0.23 for the Co-Neq bond. In all three cases, the C-N bonds in the corrin ring are stronger than the C-C bonds, and the Co-NB3 bond is weaker than the Co-N bonds in the ring. Therefore, the corrin ring has a fairly rigid perimeter with weaker bonds in the middle where the metal ion sits.

Figure 3 shows the PDOS in AdoCbl. We focus the PDOS on the following seven groups: (1) Co; (2) C α ; (3) the other atoms of Ado; (4) sp² bonded C atoms in the corrin ring;

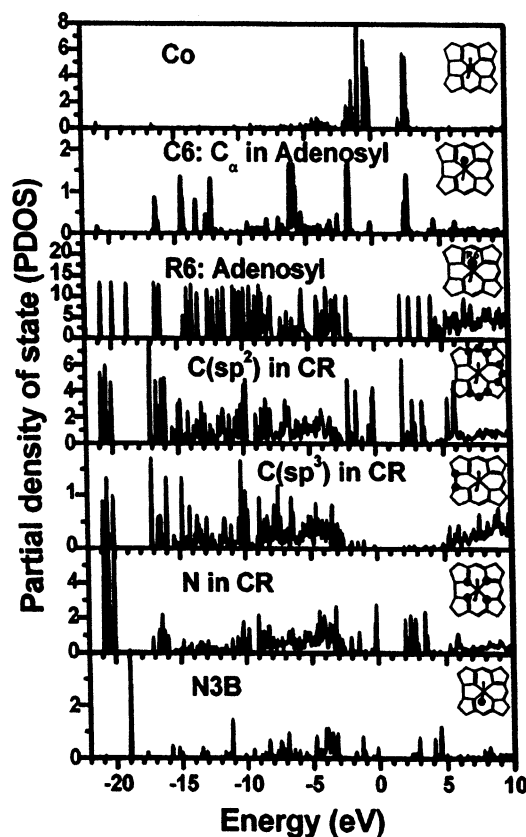


Figure 3. Calculated PDOS of AdoCbl: Co, C α , the rest of atoms in Ado, C in CR, N in CR, and N3B.

(5) sp³ bonded C atoms in the corrin ring; (6) N atoms in the corrin ring; (7) N3B atom. Similar PDOS on any atom or groups of atoms in the molecule can be obtained. The following facts are observed: (1) There is clearly a gap of about 2.0 eV separating the occupied and unoccupied Co states. The HOMO state involves the orbitals from Co, and N and C atoms in the corrin ring. From the inspection of the wave functions, it is determined that the occupied ones are the t_{2g} (xy, yz, zx) states and the unoccupied ones are the e_g states (x² - y², 3z² - r²). (2) There is very little participation of Co orbitals in the LUMO state. The LUMO state is dominated by the C-N and C-C interactions in the corrin ring and in the Ado group. (3) The PDOS for N3B and those N atoms in the corrin ring are different. The strong peaks near -19 eV are from the N 2s orbitals. This level is at a higher binding energy than the N atoms in the corrin ring. (4) The R6 panel contains all the atoms of Ado, excluding C α (see Scheme 1). Their PDOS are distributed over all energy ranges except in the top 2 eV region near

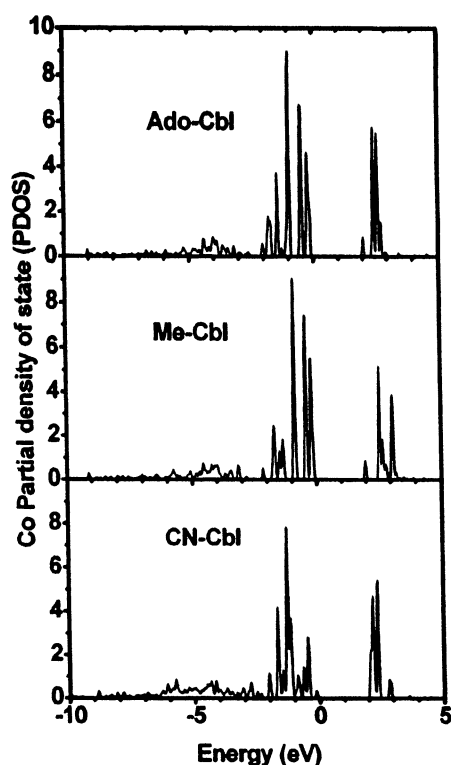


Figure 4. Comparison of PDOS of Co in AdoCbl, MeCbl, and CNCbl. The spectra are all slightly broadened.

the HOMO, where they are conspicuously absent. On the other hand, they contribute significantly to the LUMO state. The strong peaks below -18 eV in the Ado molecule come from the localized states of strong C–O and C–N bonds in the molecule. (5) In the C6, i.e., C α , panel for AdoCbl, the strong bonding peaks with the H atoms in MeCbl²⁴ are no longer present, but the Co–C bonding and the antibonding states are similar. The Co–C antibonding state in AdoCbl is at a slightly lower energy level (2.5 eV), indicating the influence of other atoms on the Co–C bond in the two molecules.

In Figure 4, we compare the PDOS of Co in AdoCbl, MeCbl, and CNCbl. It can be seen that the local PDOS for Co in AdoCbl and MeCbl are only slightly different, mainly in the unoccupied states. However, they differ quite significantly from the PDOS of Co of CNCbl. In the latter case, the HOMO state has negligible Co component. On the other hand, the LUMO state in CNCbl is significantly enhanced with Co 3d orbitals. This is consistent with the fact that the net charge on the C in CN of CNCbl is $+0.01$ compared to those for C of -0.81 and -0.58 for MeCbl and AdoCbl, respectively. It is also consistent with the much larger bond order for Co–C in the case of CNCbl.

Discussion

Comparison of the net charges for CNCbl,²² MeCbl,²³ and AdoCbl shows that they are essentially equal for all the corresponding atoms, with the exception of the C α atom (Table 3). The net charge of the latter is $+0.01$, -0.81 , and -0.58 for CNCbl, MeCbl, and AdoCbl, respectively. This result seems to reflect principally the electronic influence of the different substituents on C α (Scheme 1). However,

the nature of R does not appear to affect the net charge of the metal center or the other five N donors. This does not agree with the previous conclusions,^{14a,c} based on DFT geometry optimization of the analogous corrins, that the Ado group induced more electronic charge density on Co than Me. The net charges on the N21, N24 donor pair are slightly less negative than those on the N22, N23 donor pair, and correspondingly the Co–N21 and Co–N24 distances are shorter than the Co–N22 and Co–N23 ones.³⁰ The bond orders (BOs) are very similar for all the bonds in the three cobalamins, if the Co–C bond and a slight decrease in the Co–NB3 bond order from CNCbl to AdoCbl are excluded (Table 3). These results are consistent with the structural data^{21,22} which suggest that the change in R affects significantly only the axial distances. Furthermore, the trend in BOs within the delocalized moiety of the corrin ring (equal in the three cobalamins) reflects that of the experimental distances.^{21,22} The Co–CN BO is about twice those of the Co–Me and Co–Ado bonds, suggesting a significant Co to CN π back electron donation, i.e., a significant Co–CN double bond character. *Unexpectedly, the Co–C bond order in AdoCbl is essentially equal to or even higher than that in MeCbl.* This could contrast with experimental data, reported in Table 2 (bond lengths, BDEs, and stretching constants), which suggest that the Co–Me bond is significantly stronger than the Co–Ado bond.

It may be appropriate to compare our ab initio calculation using the OLCAO-LDA method to the recent calculation of Jensen et al.,^{14c} who have performed the DFT calculations on B₁₂ models that contain the entire corrin ring. However, all the side chains including the important nucleotide loop which contains the strongly electron negative PO₄ group were neglected. Although both calculations are based on DFT, there are significant variations in the approach, computational algorithm, exchange-correlation functional, and, most importantly, the aim of the calculation. Jensen et al.'s work focused mainly on the geometry optimization of the corrin ring with different models of the attached α -axial ligands. They used the B3LYP potential and hybrid basis functions. The accuracy of the relative energies is the most important issue in determining various bond lengths and bond angles. They showed that the HOMO–LUMO gaps of the eight models studied differ very little, in the 3.3–3.4 eV range. Unfortunately, the calculated Co–NB3 (N_{ax}) bond distance in MeCbl differs from the measured value by 0.14 Å, or 6.4%, indicating a possible deficiency in the calculation. They also found large differences in the equilibrium structure of the CNCbl model from those of MeCbl and AdoCbl. It should be noted that Jensen and Ryde have suggested that the B3LYP DF approach seems to be a problem in calculating the BDE energies in MeCbl.^{14d} This large difference could reflect the small energy differences with respect to the conformational changes in these molecules.

Andruniow, Kozłowski, and Zgierski^{14f} also used a similar method to perform time-dependent DFT calculations on some of the truncated B₁₂ models. The significance of their work is the calculation of an absorption spectrum for vitamin B₁₂,

Electronic Structure of Adenosylcobalamin

which showed good agreement with the measured data, if a shift in the energy scale is applied.

In contrast, the present study aims at the electronic structure and bonding in B₁₂ coenzymes using the highly accurate experimentally determined molecular structure. Thus, the full molecule is used, with all the side chains included in the calculation to avoid the need for geometry optimization. Using atomic basis functions and an effective orthogonalization to the core scheme, a fully self-consistent quantum mechanical calculation of this large and complex molecule was accomplished. The results enable us to understand the energy spectrum in terms of atom-resolved PDOS and the effects of charge transfer and bond strength using the effective charge and bond order calculations. Our calculated HOMO–LUMO gaps for the three cobalamins CNCbl, MeCbl, and AdoCbl are 1.96, 2.09, and 2.00 eV, respectively. They are smaller than those of ref 14c (3.38, 3.33, and 3.31 eV in the same order). This can be attributed mainly to the differences in the computational methods and to the different molecular geometries used in the respective calculations. Remarkably, both calculations show that the electronic structure of CNCbl should be significantly different from those of MeCbl and AdoCbl, and that their variations in the HOMO–LUMO gap should be small.

Finally, the efficiency and the versatility of our computational method for complex biomolecular systems have been

fully demonstrated. We expect to extend our investigations to include the presence of solvent molecules and their effects on the overall electronic structure of the B₁₂ molecules.

In conclusion, this analysis suggest that the electronic structure reflects most of the features of cobalamins, as well as the differences between them, and can be considered as a good starting base to examine the modifications induced on the Co–C bond by electronic and steric perturbations. In the case of CNCbl and MeCbl, the calculated electronic structure is in good agreement with the soft-X-ray fluorescence measurements.^{23,24} It is highly desirable that similar measurements can be extended to AdoCbl as well.

Acknowledgment. The work at Trieste is supported by the CofinLab scheme of Ministero dell'Istruzione, Università e Ricerca (MIUR), Rome, Italy. Work at UMKC was supported in part by the U.S. Department of Energy under Grant DE-FG02-84DR45170. Supercomputer time allocation at the National Energy Research Supercomputer Center (NERSC) of DOE is greatly appreciated.

Supporting Information Available: Crystallographic information in CIF format. This material is available free of charge via the Internet at <http://pubs.acs.org>.

IC0348446

Structure and bonding in a cubic phase of SiAlON derived from the cubic spinel phase of Si_3N_4

Lizhi Ouyang and W. Y. Ching^{a)}

Department of Physics, University of Missouri-Kansas City, Kansas City, Missouri 64110

(Received 18 April 2002; accepted for publication 8 May 2002)

The structure and electronic bonding in the spinel SiAlON ($\text{Si}_{6-z}\text{Al}_z\text{O}_z\text{N}_{8-z}$, $z=1$) derived from the cubic $c\text{-Si}_3\text{N}_4$ are studied by a first-principles density functional method. Al prefers the octahedral site of the spinel lattice. The small energy difference between the four possible structural configurations indicates that the real SiAlON may be a random solid solution. The lowest energy configuration of $c\text{-Si}_5\text{AlON}_7$ is a semiconductor with a direct LDA band gap of 2.29 eV. © 2002 American Institute of Physics. [DOI: 10.1063/1.1491004]

Si_3N_4 and SiAlONs are important high temperature structural ceramics with many outstanding properties.^{1,2} They have been increasingly utilized in a variety of engineering and electronic applications. In particular, the quaternary SiAlON system offers additional parameter variations that could further enhance its role as a significant industrial material where high strength, wear resistance, and chemical inertness along with special electronic and dielectric properties are required.³ A fundamental understanding of its structure and bonding is important for its successful applications. There are two well-known SiAlON systems with a hexagonal lattice structure, $\alpha\text{-SiAlON}$ and $\beta\text{-SiAlON}$, which are, respectively, derived from $\alpha\text{-}$ and $\beta\text{-Si}_3\text{N}_4$ by pair substitution of (Si, N) by (Al, O).³⁻⁵ They can be represented by the chemical formula $\text{Si}_{6-z}\text{Al}_z\text{O}_z\text{N}_{8-z}$ with z ranging from 0 to near 4. The exact sites of substitution are unknown since x-ray diffraction can hardly distinguish the variation in electron density, and it is widely believed that SiAlON is actually in the form of a solid solution. Similar pair substitution in $\text{Si}_2\text{N}_2\text{O}$ results in the so-called O'-SiAlON series.⁶

Recently, it was reported that in addition to $\alpha\text{-}$ and $\beta\text{-Si}_3\text{N}_4$, cubic Si_3N_4 ($c\text{-Si}_3\text{N}_4$) with a spinel structure could be synthesized at high temperature and pressure.⁷ An aspect of this discovery is that Si in $c\text{-Si}_3\text{N}_4$ can assume both tetrahedral and octahedral bonding, in contrast to the traditional belief that Si in Si_3N_4 is always tetrahedrally bonded. This has stimulated a flurry of both experimental⁸⁻¹⁴ and theoretical¹⁵⁻²⁰ activities in the search of additional spinel nitrides and in exploring their properties. Based on careful theoretical calculations, we predicted that other single and double spinel nitrides with cation elements from group IVB and group IVA of the Periodic Table are possible.²⁰ Some of them can possess a variety of astonishing properties. Since then, several laboratories have verified the existence of $c\text{-Si}_3\text{N}_4$, $c\text{-Ge}_3\text{N}_4$, and $c\text{-Sn}_3\text{N}_4$.^{13,14} However, until now we are not aware of any successful synthesis of double nitrides of the form AB_2N_4 . The existence of $c\text{-Si}_3\text{N}_4$ naturally leads to the speculation that cubic spinel SiAlON should also exist by analogous pair substitution. It was therefore particularly encouraging when Sekine *et al.* reported the successful synthesis of cubic SiAlON using a shock compression method.²¹ Although the precise structure

of the sample from the shock compression experiment was difficult to determine, and the sample may contain a mixture of amorphous phase, the presence of multicomponent spinel nitrides was unquestionable. Other laboratories may report similar success using this or other high-pressure techniques. Indeed, Schwarz and co-workers reported the successful synthesis and structure determination of spinel SiAlON by conversion of $\beta\text{-Si}_2\text{AlON}_2$ at a pressure of 13 GPa and a temperature of 1800 °C.²²

In this letter, we report a theoretical investigation of the low energy structures of spinel SiAlON. We restrict ourselves to the simplest case of one pair substitution, or $c\text{-Si}_{6-z}\text{Al}_z\text{O}_z\text{N}_{8-z}$, with $z=1$. In this case, there is still some symmetry left to make the calculation less demanding. The unit cell contains one formula unit of Si_5AlON_7 . After the full relaxation of the structure, the electronic structure and bonding for the $c\text{-SiAlON}$ are studied.

The spinel structure AB_2N_4 has a space group of $Fd\bar{3}m$ (No. 227). Cation A occupies the tetrahedral site 8a, and cation B occupies the octahedral site 16d while the N atoms are at the 32e site. There is one internal parameter u , which determines the position of N ions. The primitive cell (trigonal) contains two formula units (14 atoms). The positions of these 14 atoms are listed in Table I. When a pair of (Si, N) atoms is replaced by the (Al, O) pair, the symmetry is reduced. There are two possible choices for Al substitution: The A site substitution and the B site substitution. Careful symmetry analysis shows that there are two possible configurations for each case. We will label them as A1, A2 and B1, B2, respectively. For the A-site substitution, the symmetry is lowered to the space group of $T_{2d}-2$. There are only two unique sites for N. O substitution at site 7 or site 11 defines the two models A1 and A2. The symmetry is then further reduced to a space group of $C3v-5$ such that there are



FIG. 1. Primitive cell of: (a) $c\text{-Si}_3\text{N}_4$; and (b) $c\text{-Si}_5\text{AlON}_7$ (model B2). Dark (light) balls are N (Si) atoms. In (b) the gray ball is the substituted O and the central ball is the substituted Al.

^{a)}Electronic mail: chingw@umkc.edu.

TABLE I. Initial atomic positions of the four SiAlON models in the cubic spinel structure. Atoms 1,2: 8a site; 3–6: 16 d site; 7–14: 32e site.

Fractional coordinates			
1	0.0000	0.0000	0.0000
2	0.2500	0.2500	0.2500
3	0.6250	0.6250	0.6250
4	0.6250	0.6250	0.1250
5	0.1250	0.6250	0.6250
6	0.6250	0.1250	0.6250
7	0.3844	0.3844	0.3844
8	0.3844	0.3844	0.8468
9	0.8468	0.3844	0.3844
10	0.3844	0.8468	0.3844
11	0.8656	0.8656	0.8656
12	0.8656	0.8656	0.4032
13	0.8656	0.4032	0.8656
14	0.4032	0.8656	0.8656

	<i>c</i> -Si ₃ N ₄	A1	A2	B1	B2
1	Si _{tet}	Al	Al	Si ₁	Si ₁
2	Si _{tet}	Si ₁	Si ₁	Si ₂	Si ₂
3	Si _{oct}	Si ₂	Si ₂	Al	Si ₃
4	Si _{oct}	Si ₃	Si ₃	Si ₃	Si ₄
5	Si _{oct}	Si ₃	Si ₃	Si ₃	Si ₄
6	Si _{oct}	Si ₃	Si ₃	Si ₃	Al
7	N	O	N ₁	O	O
8	N	N ₁	N ₂	N ₁	N ₁
9	N	N ₁	N ₂	N ₁	N ₂
10	N	N ₁	N ₂	N ₁	N ₁
11	N	N ₂	O	N ₂	N ₃
12	N	N ₃	N ₃	N ₃	N ₄
13	N	N ₃	N ₃	N ₃	N ₄
14	N	N ₃	N ₃	N ₃	N ₅

Calculated TE (eV/cell) relative to B2	1.082	0.983	0.367	0.000	
Direct band gap (eV)	3.45	3.24	2.89	3.02	2.29

three nonequivalent N sites. For the B-site substitution, the symmetry is first lowered to the space group of D3d-5 for Al at any of the octahedral sites. Without loss of generality, we assume the substitution is at site 3 (model B1) and site 6 (model B2), with O at site 7. Again, N atoms at the 32e site split into three different types for B1 and five different types for B2, which has the lowest symmetry of all. These four

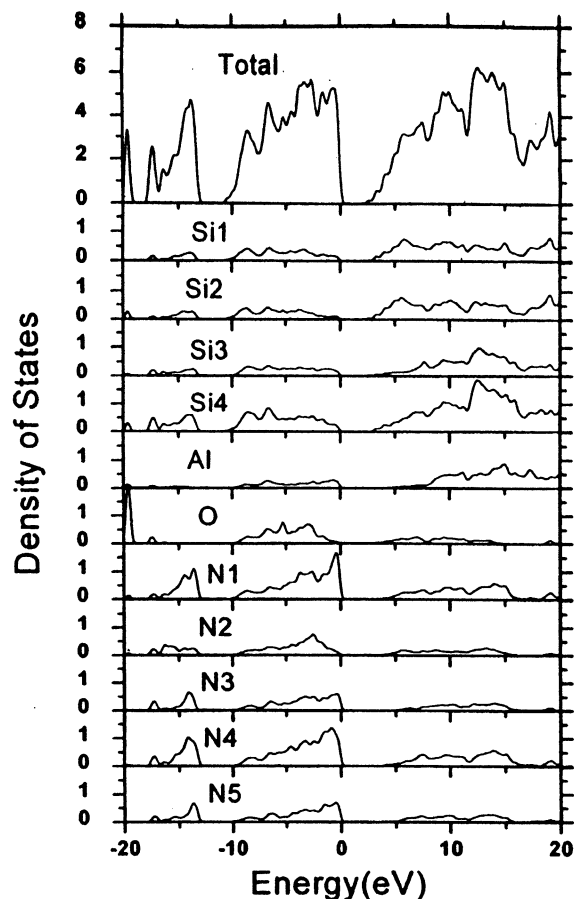
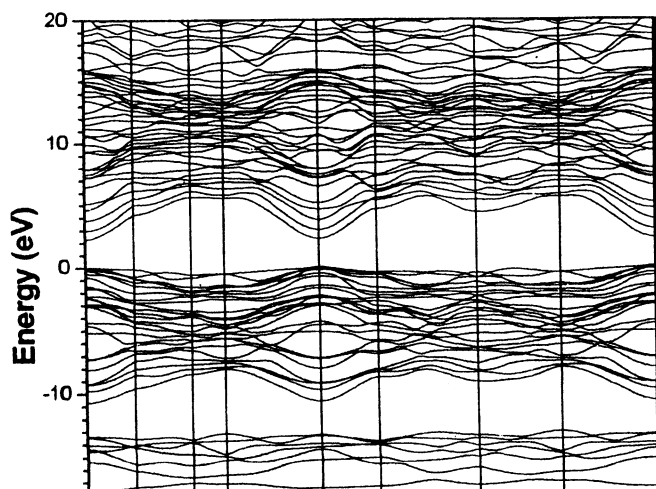


FIG. 3. Total and partial DOS of *c*-Si₅AlON₇ (model B2). Note Si₄, N₁, and N₄ have twice as many atoms.

configurations are summarized in Table I. The primitive cell of the B2 model is shown in Fig. 1.

All four initial structures were relaxed by a total energy minimization scheme^{23,24} based on the *ab initio* orthogonalized linear combination of atomic orbitals (OLCAO) method.²⁵ This is an efficient scheme that can optimize crystal geometry with the variation of both the lattice constants and internal parameters constrained only by the crystal symmetry. Of the four models, B2 has the lowest energy and A1 has the highest energy. This indicates that Al in *c*-SiAlON prefers the octahedral site to the tetrahedral site. However, the maximum difference between them is quite small, less than 0.08 eV per atom. The differences between A1, A2, and B1, B2 are even smaller. The energy differences are listed in Table I. It is entirely possible that the real *c*-SiAlON material may exist in the form of random solid solutions. We also found that the pair substitution for *z*=1 resulted in an increase of the unit cell volume by 1.11% in model B2 and 1.76% in model A1. The facts that Al prefers the octahedral site and that (Al,O) pair substitution leads to lattice expansion are fully consistent with Ref. 22.

The electronic structure of *c*-Si₅AlON₇ is calculated using the density functional-theory based OLCAO method²⁵ with a local density approximation. The same method has been used in the study of many complex crystals including *c*-Si₃N₄ and β - and α -Si₃N₄.^{15,26} The calculated band structure for model B2 is shown in Fig. 2. The total density of

TABLE II. Comparison of calculated effective charge Q^* and the average bond order (BO) in c - Si_3N_4 and c - Si_5AlON_7 (model B2). The average bond lengths (BL) are in parentheses.

	Atom	Q^* (electron)	BO (BL Å)
c - Si_5AlON_7	Si ₁	2.59	0.366 (1.805)
	Si ₂	2.48	0.349 (1.797)
	Si ₃	2.62	0.238 (1.908)
	Si ₄	2.58	0.239 (1.905)
	Al	1.66	0.200 (1.947)
	O	6.93	0.146 (1.963)
	N ₁ ×2	6.10	0.280 (1.882)
	N ₂	6.03	0.274 (1.867)
	N ₃	6.10	0.281 (1.853)
	N ₄ ×2	6.08	0.277 (1.874)
c - Si_3N_4	N ₅	6.07	0.271 (1.903)
	Si _{tet}	2.65	0.362(1.831)×4
	Si _{oct}	2.58	0.241(1.885)×6
	N	6.05	0.271(1.872)×8

gaps for the other three models are listed in Table 1. The real band gap could be somewhat larger since it is well known that LDA calculation generally underestimates the band gap. It appears that the A-site substitution results in a slightly larger band gap than the B-site substitution. c - Si_3N_4 is also a direct band gap insulator with a larger gap of 3.45 eV.¹⁵ Previous calculations of β - SiAlON with $z=1-4$ obtained smaller band gap values which are believed to be underestimated because the structures of β - SiAlON used in that calculation were not relaxed.²⁷ When a pair of (Al,O) atoms is substituted for a pair of (Si, N) atoms, the DOS becomes more complex (Fig. 3) due to the introduction of the Al-N, Al-O, and Si-O bonds. In model B2, Si₁ and Si₂ are at the tetrahedral site with Si₂ having one Si-O bond. Si₃ and Si₄ are at the octahedral site with Si₄ having one Si-O bond. The Al at the octahedral site has an Al-O bond and five Al-N bonds. For the N ions, N₂ and N₅ each have four Si-N bonds while N₁, N₃, and N₄ all have one Al-N bond and three Si-N bonds. A careful examination of the PDOS shows that the major variation is in the PDOS of the N ions. The effect of Al substitution is to introduce states near the top of the valence band (VB). The main effect of O substitution is the introduction of the Al-O bond and Si-O bonds, which affect the lowest conduction band (CB), and are responsible for the reduction in the band gap. It also introduces a deeper O 2s level at -19.5 eV. However, the overall total DOS of c - SiAlON is not much different from that of c - Si_3N_4 .¹⁵

In Table II, we list the calculated Mulliken effective charge²⁸ and bond order for model B2, and compare them with those of c - Si_3N_4 .¹⁵ In c - Si_3N_4 , Si at the tetrahedral site has a much stronger covalent bond with N than Si at the octahedral site, mainly because of the difference in the bond lengths. In addition to the fact that an Al-O bond is more ionic than a Si-N bond, in the SiAlON system, substitution of the a (Si,N) pair by a (Al,O) pair introduces a much greater variation in the bond lengths, so only the averaged bond order and BL for each atom are listed. Generally speaking, cations at the tetrahedral site have larger bond order than cations at the octahedral site, and (Al,O) have weaker bonds

crystal bond order, which is a measure of the overall bond strength of the crystal, is 8.347 for c - Si_5AlON_7 , only slightly lower than that of c - Si_3N_4 (8.670). We thus expect c - SiAlON to have a low compressibility similar to c - Si_3N_4 .

In conclusion, we have elucidated the structure and electronic properties of the new spinel SiAlON . c - SiAlON ($z=1$) is a semiconductor with a direct LDA band gap ranging from 2.29 to 3.24 eV. Since, c - SiAlON most likely exists in the form of solid solutions, this band gap can be tuned with the z value. This tunability of the band gap offers great flexibility in its potential application as a viable electronic and optoelectronic material. It is also shown that c - SiAlON retains strong covalent bonding similar to c - Si_3N_4 .

This work was supported by U.S. Department of Energy under Grant No. DE-FG02-84ER45170 and the NEDO International Grant from Japan, and partially by NSF Grant No. DMR-00162 in collaboration with NANOAM Project of EU-CODIS (G5RD-CT-2001-00586).

- ¹ Mater. Res. Soc. Symp. Proc. **287**, (1993), special issue on silicon nitride ceramics edited by I. W. Chen, P. F. Becher, M. Mitomo, G. Petzow, and T.-S. Yen.
- ² *Silicon Nitrides 93*, edited by M. J. Hoffmann, P. F. Becher, and G. Petzow. (Trans. Tech., Switzerland, 1994); W.-Y. Ching, S.-D. Mo, I. Tanaka, and M. Yoshiya, Phys. Rev. B **63**, 064102 (2001).
- ³ T. Ekström and M. Nygren, J. Am. Ceram. Soc. **75**, 259 (1992).
- ⁴ L. L. K. Falk, Z.-J. Shen, and T. Ekström, J. Eur. Ceram. Soc. **17**, 1099 (1997).
- ⁵ X. Jiang, Y.-K. Baek, S.-M. Lee, and S.-J. L. Kang, J. Am. Ceram. Soc. **81**, 1907 (1998).
- ⁶ M. E. Bowden, G. C. Barris, and I. W. M. Brown, J. Am. Ceram. Soc. **81**, 2188 (1998).
- ⁷ A. Zerr, G. Miede, G. Serghiou, M. Schwarz, E. Kroke, R. Riedel, H. Fuess, P. Kroll, and R. Boehler, Nature (London) **400**, 340 (1999).
- ⁸ T. Sekine, H. He, T. Kobayashi, M. Zhang, and F. Xu, Appl. Phys. Lett. **76**, 3706 (2000).
- ⁹ J. Z. Jiang, K. Stahl, R. W. Berg, D. J. Frost, T. J. Zhou and P. X. Shi, Europhys. Lett. **51**, 62 (2000).
- ¹⁰ K. Leinenweber, M. O'Keefe, M. S. Somayazulu, H. Hubert, P. F. McMillan, and G. H. Wolf, Chem.-Eur. J. **5**, 3076 (1999).
- ¹¹ G. Serghiou, G. Miede, O. Tschauner, A. Zerr, and R. Boehler, J. Chem. Phys. **111**, 4659 (1999).
- ¹² I. Tanaka, T. Mizoguchi, T. Sekine, H. He, K. Kimoto, T. Kobayashi, S.-D. Mo, and W. Y. Ching, Appl. Phys. Lett. **78**, 2134 (2001).
- ¹³ E. Soignard, M. Somayazulu, J. Dong, O. F. Sankey, and P. F. McMillan, J. Phys.: Condens. Matter **13**, 557 (2001).
- ¹⁴ M. Shemkunas, W. T. Petuskey, and G. H. Wolf, J. Am. Ceram. Soc. **85**, 101 (2002).
- ¹⁵ S.-D. Mo, L. Ouyang, W. Y. Ching, I. Tanaka, Y. Koyama, and R. Riedel, Phys. Rev. Lett. **83**, 5046 (1999).
- ¹⁶ J. E. Lowther, Phys. Rev. B **60**, 11943 (1999).
- ¹⁷ W. Y. Ching, S.-D. Mo, L. Ouyang, I. Tanaka, and M. Yoshiya, Phys. Rev. B **63**, 064102 (2001).
- ¹⁸ W. Y. Ching, S.-D. Mo, L. Ouyang, I. Tanaka, and M. Yoshiya, Phys. Rev. B **61**, 10609 (2000).
- ¹⁹ W. Y. Ching, S.-D. Mo, and L. Ouyang, Phys. Rev. B **63**, 245110 (2001).
- ²⁰ W. Y. Ching, S.-D. Mo, Y. Chen, and P. Rulis, J. Am. Ceram. Soc. **85**, 75 (2002).
- ²¹ T. Sekine, H. He, T. Kobayashi, M. Tansho, and K. Kimoto, Chem. Phys. Lett. **344**, 295 (2001).
- ²² M. Schwarz, A. Zerr, E. Kroke, G. Miede, I.-W. Chen, M. Heck, B. Thybusch, B. T. Poe, and R. Riedel, Angew. Chem. Int. Ed. Engl. **41**, 789 (2002).
- ²³ W. Y. Ching, L. Ouyang, and J. Gale, Phys. Rev. B **61**, 8696 (2000).
- ²⁴ L. Ouyang and W. Y. Ching, J. Am. Ceram. Soc. **84**, 801 (2001).
- ²⁵ W. Y. Ching, J. Am. Ceram. Soc. **73**, 3135 (1990).
- ²⁶ Y.-N. Xu and W. Y. Ching, Phys. Rev. B **51**, 17379 (1991).
- ²⁷ W. Y. Ching, M.-Z. Huang, and S.-D. Mo, J. Am. Ceram. Soc. **83**, 780 (2000).

Structure and chemical bonding

YUNUSOV¹, L. OUYANG³, L. RANDACCIO⁴, J. RUSLIS³,
and M. NEUMANN⁵

¹ Russian Academy of Science-Ural Division,
610010, Russia

² Engineering Physics, University of Saskatchewan,
Saskatchewan S7N 5E2, Canada

³ University of Missouri-Kansas City
Department of Chemistry,
Trieste, Italy

⁴ Fachbereich Physik - D-49069 Osnabrück,
Germany

Received in final form 13 March 2003

Abstract. The structure and chemical bonding of vitamin B₁₂ (cyanocobalamin) are studied by means of X-ray emission (XES) and X-ray absorption (XAS) spectroscopy. The obtained results are compared with the results of *ab initio* electronic structure calculations. The combination of the orthogonalized linear combination of atomic orbitals (OLCAO) method with the density functional theory (DFT) method allows us to study the chemical bonding in vitamin B₁₂ in detail. It is shown that the Co-N bond is weaker than the Co-C bond. It is further confirmed that the Co-C bond is stronger than that of methylcobalamin resulting from the homolytic cleavage of the Co-C bond.

Vitamin B₁₂ (cyanocobalamin, CN-Cbl) is a red crystalline compound with a physiological function itself [1]. It belongs to a class of cobalt-containing compounds, the amide side chains, labeled *a-g* in fig. 1, which are coordinated to the central cobalt atom. This ligand occupies the fifth coordination site of an octahedral cobalt atom. The other five coordination sites are occupied by a 5'-deoxyadenosyl group (Ado-Cbl) with R=5'-deoxyadenosyl group (Ado-Cbl) with R=CH₂. It is supposed that the Ado-Cbl derivatives are intimately connected with the biological functions of vitamin B₁₂. Their abilities to bind proteins and substrates are different. The Ado-Cbl derivatives interact differently via which vitamin B₁₂-forms are available for biological processes.

The electronic structure of CN-Cbl and CH₃-Cbl molecules (C₆₃H₈₈O₁₄N₁₄PCo and C₆₃H₉₁O₁₄N₁₃PCo, respectively) including all side chains were calculated using the density functional theory based *ab initio* orthogonalized linear combination of the atomic orbital method (OLCAO) (see ref. [9]) in the framework of the local density approximation (LDA).

The electronic structure of CN-Cbl and CH₃-Cbl molecules (C₆₃H₈₈O₁₄N₁₄PCo and C₆₃H₉₁O₁₄N₁₃PCo, respectively) including all side chains were calculated using the density functional theory based *ab initio* orthogonalized linear combination of the atomic orbital method (OLCAO) (see ref. [9]) in the framework of the local density approximation (LDA).

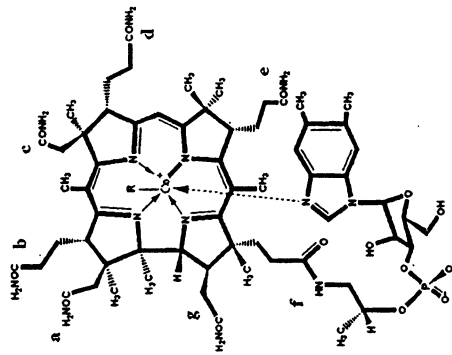


Fig. 1

Fig. 1 - Sketch of the vitamin B₁₂ molecule with seven side chains labeled a, b, c, d, e, f, and g.

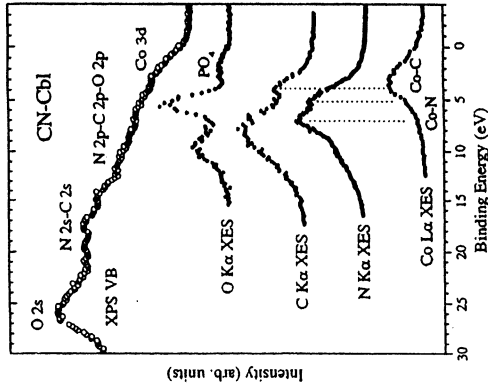


Fig. 2

Fig. 2 - Comparison of X-ray emission and photoelectron spectra of CN-Cbl on the binding energy scale.

50% decreased Co-C bond strength and corresponding rate enhancement for the homolytic cleavage due to a half-filled antibonding σ^* (Co-CH₃) orbital (d_z^2 component). The homolytic bond cleavage leads to paramagnetic Co(II) with a low-spin d^7 configuration (one unpaired electron) and a primary alkyl radical.

In the present paper we report X-ray fluorescence measurements of vitamin B₁₂ (CN-Cbl) and B₁₂-derivative (CH₃-Cbl) performed to study the electronic structure and chemical bonding of these cobalt complexes. The obtained results are compared with first-principles electronic structure calculations, which include all side chains. The previous theoretical calculations were all based on simpler models in which side groups were replaced by the H atoms [4-7].

The non-resonant carbon, nitrogen and oxygen $K\alpha$ ($2p \rightarrow 1s$ transition) and cobalt $L_{2,3}$ ($3d_{5/2} \rightarrow 2p$ transition) soft X-ray emission spectra (XES) were measured at beamline 8.0 of the Advanced Light Source at Lawrence Berkeley National Laboratory and its X-ray fluorescence endstation [8]. The excitation energy of the incident photons is tuned to 300, 430, 540 and 840 eV in order to excite non-resonantly C $K\alpha$, N $K\alpha$, O $K\alpha$ and Co $L_{2,3}$, the soft X-ray emission spectra (XES), respectively. Carbon, nitrogen and oxygen $K\alpha$ spectra were measured with an energy resolution of 0.3-0.4 eV, for cobalt $L_{2,3}$ XES the energy resolution was 0.7-0.8 eV.

The XPS measurements were performed with an ESCA spectrometer of Physical Electronics (PHI 5600 ci, with monochromatized Al- $K\alpha$ radiation of a 0.3 eV FWHM). The energy resolution of the analyzer was 1.5% of the pass energy. The pressure in the vacuum chamber during the measurements was below $5 \cdot 10^{-9}$ mbar.

The electronic structure of CN-Cbl and CH₃-Cbl molecules (C₆₃H₈₈O₁₄N₁₄PCo and C₆₃H₉₁O₁₄N₁₃PCo, respectively) including all side chains were calculated using the density functional theory based *ab initio* orthogonalized linear combination of the atomic orbital method (OLCAO) (see ref. [9]) in the framework of the local density approximation (LDA).

The exchange-correlation potential used is the Wigner-Interpolation formula. Details of the calculation will be presented elsewhere and we only briefly outline the steps of the calculation. The molecular orbitals are expanded in atomic orbitals consisting of Gaussians. A full basis set consisting of Co ([Ar] 4s, 4p, 3d, 5s, 5p, 4d), C, N, O (1s, 2s, 2p, 3s, 3p), P ([Ne] 3s, 3p, 4s, 4p, 3d), and H (1s, 2s, 2p) atomic orbitals was adopted. The LDA potential was expressed as a superposition of atom-centered functions also consisting of Gaussians. All the multi-center integrals occurring in the Hamiltonian and overlap matrices were evaluated in the direct space with no approximation to the range of interaction. Diagonalization of secular equation after the potential iterated to self-consistency gave the energy eigenvalues and molecular wave functions. A special advantage of the OLCAO method is the ease with which the energy spectra can be presented in the form of total density of states (DOS) and the atom- and orbital-resolved partial DOS (PDOS). The PDOS can present the complicated inter-atomic and intermolecular interactions of specific functional groups in a simple graphic form, and is necessary for the interpretation of the experimental spectra. This is particularly important for complex molecules such as B₁₂ enzymes.

In the case of non-resonant excitation, the spectral shape of X-ray emission can be described with the emission decoupled from the excitation. The electron undergoes a transition from a valence level to fill the core hole created by the incident photon absorption. Excitation and emission are both governed by the dipole selection rule, $\Delta l = \pm 1$, which means that the 1s core level holes in carbon, nitrogen and oxygen atoms can only be filled by p valence electrons. For L-emission of cobalt, the 2p core level holes are filled by 3d and 4s valence electrons. Therefore, X-ray emission spectra (XES) probe the local PDOS at each particular atomic site. X-ray transitions are localized within the first coordination sphere of emitting atoms and in this respect X-ray emission spectra present an ideal tool for studying the local environment and local chemical bonding of selected atoms in complicated molecular systems such as vitamin B₁₂. In order to determine the mixing of electronic states of the constituents, the X-ray emission spectra are converted to the binding energy scale which is realised using XPS binding energies of the core levels.

The comparison of XPS VB (probing total DOS) with C K_α, N K_α, O K_α and Co L_{2,3} XES (probing partial DOS) of CN-Cbl is presented in fig. 2. In order to convert C K_α, N K_α, O K_α and Co L_{2,3} XES to the binding energy scale we have used XPS C 1s (285.35 eV), N 1s (399.89 eV), O 1s (532.29) and Co 2p_{3/2} (780.25 eV) binding energies. The oxygen, nitrogen and carbon 2p-states are situated in the middle of the valence band overlapping in binding energy. This is in accordance with the chemical structure of CN-Cbl (fig. 1), according to which one can expect strong C-N and C-C interactions and a mixing of C 2p and N 2p-states. The Co L₃-emission coincides with the first feature of C K_α XES on the binding energy scale showing that the Co-C bonds are strong. On the other hand, the intensity maxima of N K_α XES are overlapped only with the tail of Co L₃ XES evidencing that the Co-N bonds are much weaker than Co-C bonds in CN-Cbl. According to XPS VB, the oxygen, nitrogen and carbon 2s-states are situated at the bottom of the valence band. These states are not seen in oxygen, nitrogen and carbon K_α XES because 2s → 1s transitions are forbidden by the dipole selection rules. The Co 3d-states are located at the top of the valence band which gives rise to a positive charge on the Co-atom in cyanocobalamin.

In fig. 3 the carbon, nitrogen and oxygen K_α XES of CN-Cbl are compared with spectra of CH₃-Cbl on the emission energy scale. The C K_α emission feature centered at 281.6 eV is responsible for the Co-C bond and has higher intensity for CN-Cbl than for CH₃-Cbl. This means that Co-C bond in cyanocobalamin is stronger than that of methylcobalamin accounting for their different biological activity. This is in accordance with the calculation of the bond order (BO) (related to a qualitative measure of the strength of a specific bond in CN-Cbl

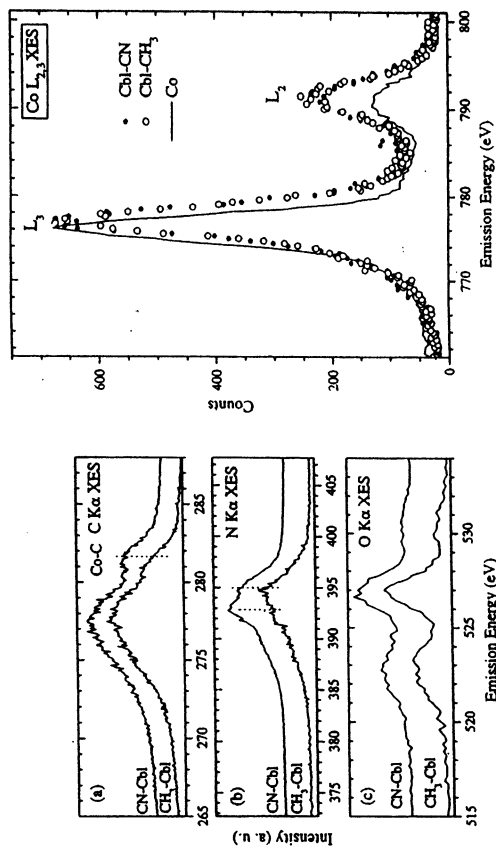


Fig. 3

Fig. 3 - X-ray emission spectra (XES) of constituents of CN-Cbl and CH₃-Cbl: (a) C K_α XES, (b) N K_α XES and (c) O K_α XES.

Fig. 4 - Co L_{2,3} XES of CN-Cbl, CH₃-Cbl and pure Co metal.

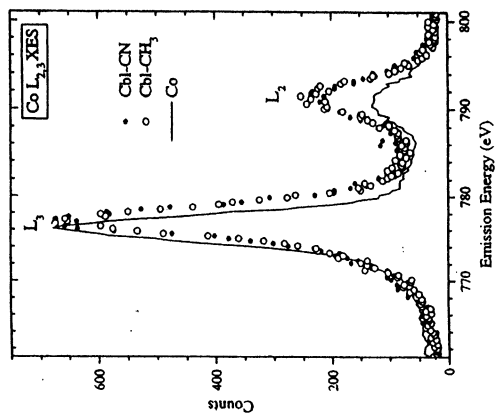


Fig. 4

molecule), which was made in ref. [10] and shows that the BO for Co-CN is 0.25, larger than the BO of Co-N in the corrin ring (0.21). It is almost two times higher than those obtained for CH₃-Cbl (0.125) and Ado-Cbl (0.151) (see ref. [11]). This is also in agreement with the experimental values of the Co-C distances, which are 1.886(4) Å in CN-Cbl and 1.979(4) Å in CH₃-Cbl [12]. Therefore, the relatively strong Co-C bond in CN-Cbl can be considered as one of the reasons why CN-Cbl is biologically inactive, in contrast to its coenzymes CH₃-Cbl and Ado-Cbl.

Nitrogen K_α XES exhibits two features at 392.7 and 394.9 eV, with the relative intensity being different for CN-Cbl and CH₃-Cbl. These differences can be attributed to the additional contribution of the CN-ligand to the formation of peak at 392.7 eV of N K_α XES for CN-Cbl. The fine structure of oxygen K_α XES of CN-Cbl and CH₃-Cbl is found to be very similar because both compounds consist of the same oxygen atoms on the amide side chains and OH groups in the sugar part of the nucleotide (fig. 1). We attribute the weak O K_α emission feature at 532 eV to the contribution of the PO₄-group.

In fig. 4 the Co L_{2,3} XES of CN-Cbl and CH₃-Cbl are presented. L_{2,3} XES corresponds to 3d4s → 2p_{1/2,3/2} dipole transitions and the ratio of L₂ to L₃ emission lines $I(L_2)/I(L_3)$ should be the same for all 3d-elements and close to the statistical value of 1/2. It is found though that this ratio is much smaller in pure 3d-metals due to strong Coster-Kronig processes of the kind L₂L₃M_{4,5} [13, 14]. The probability for non-radiative L₂L₃M_{4,5} Coster-Kronig transitions is lower for 3d oxides than for metals [15] due to the localized character of d-states and the absence of electron-hole pairs near the Fermi level as well as due to collective 3d electron excitations [16]. It has been shown that the $I(L_2)/I(L_3)$ ratio can be used as a tool for the determination of the oxidation state of 3d-ions in compounds [10]. Figure 4 shows that the ratio

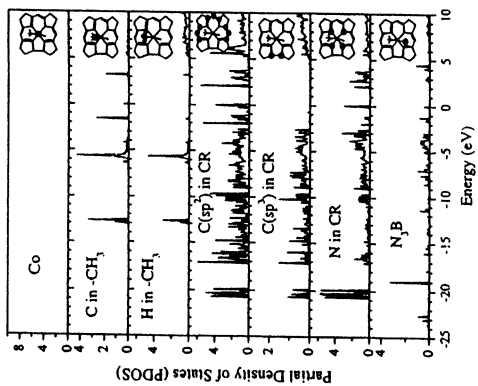


Fig. 5

Fig. 5 - The calculated PDOS of $\text{CH}_3\text{-Cbl}$: Co; C in CH_3 ; H in the CH_3 , sp^3 C in CR, sp^3 C in CR, N in CR and N in benzimidazole ligand.

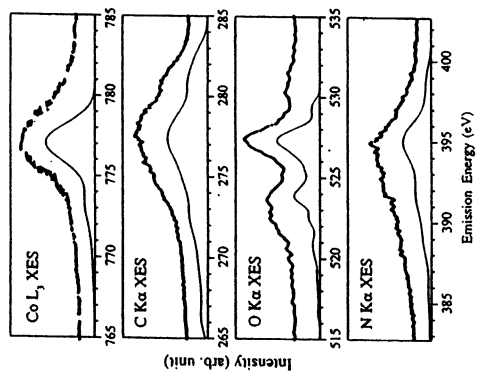


Fig. 6

Fig. 6 - Comparison of the orbital-resolved PDOS (solid lines) (for the atom) with the measured soft-X-ray emission spectra (circles) for Co L_3 , C K_{α} , N K_{α} and O K_{α} XES.

$I(L_2)/I(L_3)$ for CN-Cbl and $\text{CH}_3\text{-Cbl}$ (0.34) is two times higher than that of pure metal (0.16) and close to that of LiCoO_2 (see ref. [17]) indicating that Co is trivalent in both compounds. Figure 5 shows the calculated PDOS in $\text{CH}_3\text{-Cbl}$ for seven groups of atoms including the Co, the C in the CH_3 group, the H in CH_3 group, C atoms in the CR (nine of them are sp^2 -bond and two of them are sp^3 -bond), the four N in the *corrin ring* (CR) and the axial N in the 5th ligand. Similar PDOS can be obtained for any atom or group of atoms. The major observations can be summarized as follows: 1) Considering the Co and CR as a special unit, there is a HOMO-LUMO gap of 2.09 eV (1.96 eV for CN-Cbl). 2) The HOMO and LUMO states are dominated by C and N atoms in the CR. 3) The HOMO state also has a fair participation of Co 3d orbitals, but not the LUMO states. In the case of CN-Cbl , Co does not contribute to the HOMO states. 4) The PDOS for N_3B and N in the CR are quite different. 5) The states derived from the CH_3 group are far away from the HOMO-LUMO gap and consist of very sharp peaks in the PDOS. 6) As in all our B_{12} molecular calculations, a surprising feature is the location of molecular orbital levels derived from the phosphate PO_4 unit (not shown). Several such levels fall within the HOMO-LUMO gap of the CR, which causes the convergence in the calculation to be very slow. Since the PO_4 unit in the f side chain (fig. 1) is physically far away from the *corrin* moiety, these isolated localized states do not interact in any way with the states of the CR or Co and the gap value is defined by the states of the CR. In fig. 6, we compare the measured XES for $\text{CH}_3\text{-Cbl}$ with the orbital-resolved PDOS. The theoretical curves are the symmetry-projected portions of the PDOS of fig. 5 (s and d for Co, p for C, N, and O) suitably broadened to mimic the experimental curve. The agreement is very good. The asymmetric nature of the Co L_3 peak is well reproduced. The agreement in the multiple-peak structure of the O- K edge is impressive. It should be also

pointed out that the C- K and N- K edges consist of the sum of different C atoms in the CR and different N atoms bonded to Co. It is possible to further resolve the spectra to different contributions from atoms at different sites.

To summarize, the electronic structure of the complex vitamin B_{12} molecule has been calculated. The calculations include all side chains. The theoretical results are compared with our spectroscopic measurements and it is found that the electronic-structure calculations are fully consistent with the XES and XPS experiments. This demonstrates that the experimental and theoretical studies can be very effective in analyzing the electronic structure and chemical bonding in complex biomolecular systems. Such studies are vitally needed for progresses in molecular biochemistry to gain insights on physiological functions of specific enzymes. We plan to extend the current study to other important biomolecular systems and to explore the dynamics of the unoccupied states in such systems.

Funding by the Russian Foundation for Basic Research (Project 00-15-96575), and the Natural Sciences and Engineering Research Council of Canada (NSERC) is gratefully acknowledged. Work at UMKC was supported in part by US Department of Energy and by the NEDO International grant of Japan. The work at Trieste is supported by the Ministero dell'Università e della Ricerca (MIUR), PRIN MM03185591, and by the Consiglio Nazionale delle Ricerche (CNR), Agenzia 2000.

REFERENCES

- [1] ELLENBOGEN L. and COOPER B. A., in *Handbook of Vitamins*, edited by MACHLIN L. J. (Marcel Dekker, New York-Basel) 1991, p. 491.
- [2] BANERJEE R. (Editor), *Chemistry and Biochemistry of B₁₂* (John Wiley & Sons, New York) 1999.
- [3] GUGGER P., WILLIS A. C. and WILD S. B., *J. Chem. Soc., Chem. Commun.* (1990) 1169.
- [4] ANDRUNIOW T., ZGIERSKI M. Z. and KOZLOWSKI P. M., *J. Am. Chem. Soc.*, **123** (2001) 2679; *J. Phys. Chem. B*, **104** (2000) 10921.
- [5] ANDRUNIOW T., KOZLOWSKI P. M. and ZGIERSKI M. Z., *J. Phys. Chem.*, **115** (2001) 7522.
- [6] RANDACCIO L., GEREMIA S., NARDIN G., STENER M., TOFFOLI D. and ZAGRANNO E., *Eur. J. Inorg. Chem.*, No. 1 (2002) 93.
- [7] JENSEN K. P., SAUR S. P. A., LILJEFORS T. and NORRBY P. O., *Organometallic*, **20** (2001) 550.
- [8] JIA J. J., CALCOTT T. A., YURKAS J., ELLIS A. W., HIMPSEL F. J., SAMANT M. G., STÖHR J., EDERER D. L., CARLISLE J. A., HUDSON E. A., TERMINELLO L. J., SHUH D. K. and PERERA R. C. C., *Rev. Sci. Instrum.*, **66** (1995) 1394.
- [9] CHING W. Y., *J. Am. Ceram. Soc.*, **73** (1990) 3135.
- [10] KURMAEV E. Z., MOEWES A., GALAKHOV V. R., EDERER D. L. and KOBAYASHI T., *Nucl. Instrum. Methods B*, **168** (2000) 395.
- [11] OUYANG L., RULIS P., CHING W. Y., NARDIN G. and RANDACCIO L., to be published.
- [12] RANDACCIO L., FURLAN M., GEREMIA S., ŠLOUF M., SRNOVA I. and TOFFOLI D., *Inorg. Chem.*, **39** (2000) 3403.
- [13] MCGUIRE E. J., *Phys. Rev. A*, **5** (1972) 1043.
- [14] HOLLIDAY J. E., *J. Appl. Phys.*, **33** (1962) 3259.
- [15] GALAKHOV V. R., KURMAEV E. Z. and CHERKASHENKO V. M., *Izv. AN SSSR, Ser. Fiz.*, **49** (1985) 1513.
- [16] GREBENNIKOV V. I., GALAKHOV V. R., FINKELSTEIN L. D., OYEBCHKINA N. A. and KURMAEV E. Z., to be published in *Russian J. Solid State Phys.*, June (2003).
- [17] GALAKHOV V. R., Dr. Sci. Habil. Thesis, Institute of Metal Physics, Yekaterinburg, Russia (2002).